Lowland Technology International 2020; 22 (1): 113-122
International Association of Lowland Technology (IALT): ISSN 1344-9656
Special Issue on: Engineering Geology and Geotechniques for Developing Countries

Research Paper

Implementing the Sendai Framework in developing countries using remote sensing techniques for the evaluation of natural hazards

M.R.Z. Whitworth [1], S.J. Boulton [2] and J.N. Jones [3]

ARTICLE INFORMATION

Article history:

Received: 21 December, 2019
Received in revised form: 10 March, 2020
Accepted: 15 March, 2020
Publish on: 06 June, 2020

Keywords:

Sendai Framework
Disaster Risk Reduction
Remote Sensing
Open Source Data
Hazard
Landslide

ABSTRACT

The UNISDR Sendai Framework for Disaster Risk Reduction has the stated outcome for "The substantial reduction of disaster risk and losses in lives, livelihoods and health and in the economic, physical, social, cultural and environmental assets of persons, businesses, communities and countries". Priority 1 of the Framework, understanding disaster risk, requires policies and practices for disaster risk management to be based on an understanding of disaster risk in all its dimensions of vulnerability, capacity, exposure of persons and assets, hazard characteristics and the environment. In addition, complementary schemes such as the Millennium Challenge Corporation, 100 Resilient Cities and the UNISDR Disaster Resilient Scorecard also have an essential requirement to identify, understand, and use current and future risk scenarios. As natural hazards are a common catalyst for disaster risk, understanding current and future risk scenarios requires detailed preliminary appraisals of natural hazard and risk scenarios, both at local and national levels, as detailed in the Sendai Framework. However, due to the data-intense nature of such appraisals, undertaking them can be expensive and time consuming, and thus hinder progress at meeting the aims of Priority 1. As such, we here evaluate the potential of available "Open Source" data, such as ASTER/SRTM Digital Elevation Models (DEMs) and Landsat/Sentinel satellite imagery, coupled with a range of processing techniques, for the cost and time effective screening and preliminary assessment of a range of natural hazards. Despite the spatial resolution of these data being between 30 – 50 m, the outputs provide an important preliminary assessment of natural hazards, thus enabling policies and practices for disaster risk management to be focused on areas of high susceptibility and vulnerability. These methods are applicable to communities across the globe, but particularly to those within developing countries that may be lacking alternative data sources.

[1] Principal Engineering Geologist/Geomorphology and Corresponding Author, AECOM, East Wing Plumer House, Tailyour Road, Plymouth, PL6 5DH and School of Geography, Earth and Environmental Sciences, University of Plymouth, Drake's Circus, Plymouth, PL4 8AA, UK, michael. whitworth@aecom.com
[2] Associate Professor, School of Geography, Earth and Environmental Sciences, University of Plymouth, Drake's Circus, Plymouth, PL4 8AA, UK, Sarah.boulton@plymouth.ac.uk
[3] Ph.D Student, School of Environmental Sciences, University of East Anglia, Norwich Research Park, NORWICH, NR4 7TJ, and School of Geography, Earth and Environmental Sciences, University of Plymouth, Drake's Circus, Plymouth Joshua.N.Jones@uea.ac.uk
Note: Discussion on this paper is open until December 2020

M.R. Z. Whithworth et al. / Lowland Technology International 2020; 22 (1): 113-122
Special Issue on: Engineering Geology and Geotechniques for Developing Countries

1. Introduction

A disaster is defined as a situation or event that overwhelms local capacity, necessitating a request at national or international level for external assistance; often in response to an unforeseen or sudden event that causes great damage, destruction and human suffering (CRED/UNISDR 2017). Whilst disasters can rarely be considered truly natural (e.g. Hartman et al., 2006), natural-hazards are a common catalyst of disaster. Natural hazards can be subdivided into climate related hazards (e.g. floods, storms, droughts), which are considered to be predominantly controlled by climatic processes, and geohazards (e.g. earthquakes, landslides, tsunamis), which are considered to be predominantly controlled by geophysical processes. Between 1998 and 2017, over 7,000 natural hazard related disasters are estimated to have caused 1.3 million fatalities, impacted over 4.4 billion people and caused economic losses in excess of USD 2,908 billion. Of these 7000 disasters, 91% are attributable to climate-related hazards, of which 43% are attributable to floods that affected over 2 billion people. The economic losses due to climate-related hazards are estimated to be in excess of USD 2,245 billion (CRED/UNISDR, 2017).

In 2015 the UN Sendai Framework was ratified with the stated aim to "substantially reduce disaster risk and losses in lives, livelihoods and health and in the economic, physical, social, cultural and environmental assets of persons, businesses, communities and countries." Subsequently, in 2016, the UN Secretary-General launched "The Sendai Seven Campaign" to promote seven targets over seven years. These targets include;

(a) "aiming to lower average per 100,000 global mortality between 2020 and 2030 compared to 2005-2015", and;

(b) "substantially reduce the number of affected people globally by 2030".

(c) "Reduce direct disaster economic loss in relation to global gross domestic product (GDP) by 2030."

These targets relate to Priority 1 of the Sendai Framework; understanding disaster risk, which requires policies and practices for disaster risk management to be based on an understanding of disaster risk in all its dimensions of vulnerability, capacity, exposure of persons and assets, hazard characteristics and the environment. In addition, holistic community wide schemes such as the Millennium Challenge Corporation, 100 Resilient Cities and the UNISDR Disaster Resilient Scorecard have an essential requirement to identify, understand and use current and future risk scenarios in line with Priority 1 of the Sendai Framework (UN, 2015). As outlined above, natural hazards are intrinsically linked to disaster risk, so meeting the aims of Priority 1 requires detailed preliminary appraisals of natural hazard and risk scenarios, both at local and national levels. However, owing to the data-intense nature of such appraisals, they can be relatively expensive and time consuming, and thus hinder progress at meeting the aims of Priority 1.

Therefore, in this paper we evaluate the potential of available "Open Source" data, such as ASTER/SRTM Digital Elevation Models (DEMs) and Landsat/Sentinel satellite imagery, coupled with a range of processing techniques, for a cost and time effective preliminary appraisal of a range of impacts stemming from natural hazards. Whilst such techniques are applicable anywhere, we consider them of particular use to the developing world, which is more likely to be lacking alternative data sources.

Case studies herein focus on: A) the use of Landsat satellite imagery in the analysis of historical landslide occurrence along the Araniko Highway, Nepal, where data covering a period of almost 30 years is available. B) The role of Sentinel-2 data in an urban setting (Kathmandu) where land use classification coupled with DEM-determined drainage models and geological data are utilised to investigate the range of susceptibility factors that may impact urban resilience. C) The application of digital data sets in a coastal environment (Myanmar) with the focus on flood hazard and risk. This case study is of particular importance because, as outlined above, flooding is a major contributor to natural hazard vulnerability in the developing world. D) The use of DEMs in the identification of active faulting and the extraction of landscape metrics that can be used to quantify uplift and erosion in vulnerable landscapes.

2. Landslide mapping in Nepal using Landsat imagery

In Nepal, landslides are a major cause of fatality and economic loss (Petely et al., 2007), with landslides impacting urban environments, the rural agricultural economy and road/trekking infrastructure (e.g. Xu et al., 2017; Jones et al., 2019). As such, an improved understanding of landslide hazard and risk should be considered necessary for Nepal to meet the targets outlined in the Sendai Framework. However, improving our understanding of landslide hazard requires comprehensive landslide inventories across a range of scales and environments. Obtaining such landslide data for Nepal is non-trivial. Field-based mapping is expensive and time consuming, whilst traditional aerial photograph based remote mapping is limited by a lack of available

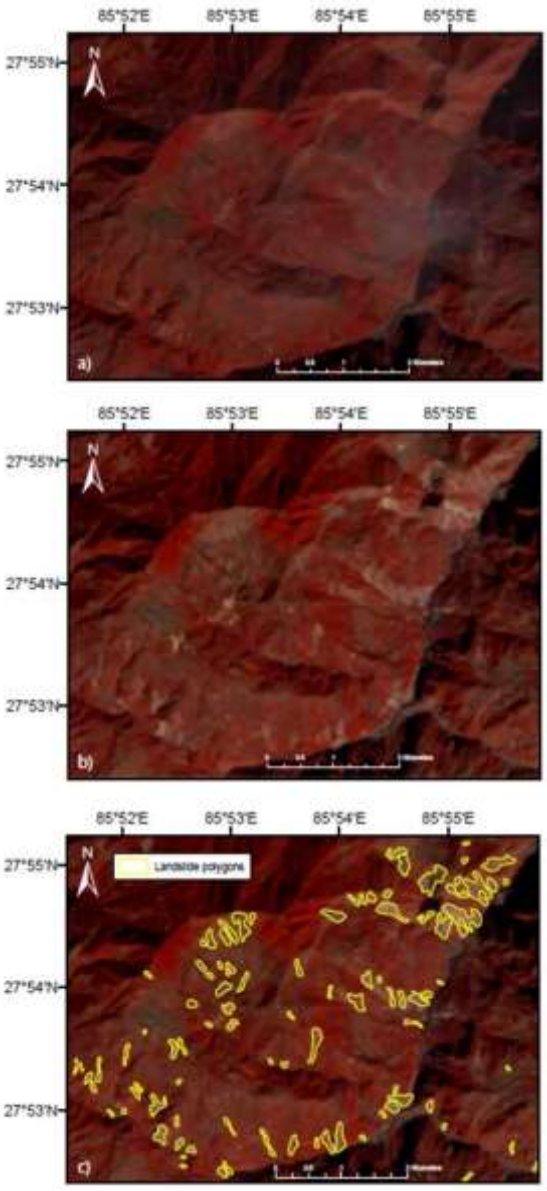

Fig. 1. Panels demonstrating how Landsat 8 imagery (bands NIR/G/B) can be used to delineate fresh landslides. a) Pre-2015 Gorkha earthquake imagery acquired on 24/01/2015, b) Post-2015 Gorkha earthquake acquired on 12/02/2016, c) The same imagery as in b), but with fresh landslides delineated as individual polygons.

imagery. However, recent freely-available satellite imagery such as Landsat now provides an opportunity for widespread, relatively rapid, landslide mapping.

In 2008, the U.S Geological Survey (USGS) made all imagery from the Landsat program freely available to the public (Woodcock et al., 2008). The Landsat satellite program is a joint NASA/USGS project which has been acquiring data since the Earth Resources Technology Satellite 1, since renamed Landsat 1, was launched in 1972. Since then, seven further satellites have been launched, making the Landsat program the longest continuously-acquired space-based archive of the Earth's surface. As such, these data are a potentially excellent resource for large-scale mapping of landslides over the past 30 years in regions such as Nepal that lack widespread aerial photographs.

2.1 The Landsat satellite data

Landsat satellites 1/2/3 cover the period of 1972 to 1983, have a maximum temporal resolution of 18 days, and a maximum spatial resolution of 40 m. However, in our experience, their spatial coverage over Nepal is very poor, making them insufficient for landslide mapping here. Landsat satellites 4/5 cover the period 1982 - 2013, have a maximum temporal resolution of 16 days and a maximum spatial resolution of 30 m. In Nepal, they provide a good spatial coverage of data from 1987, making them ideal for the mapping of medium-large landslides over the past 30 years. Landsat 7 was launched in 2003 and can be resampled to produce optical imagery with a spatial resolution of 15 m and a temporal resolution of 16 days. However, this satellite suffered a Scan Line Corrector (SCL) failure which reduces the data coverage of each image by 22%, rendering the imagery less effective for accurate landslide mapping. Landsat 8 was launched in 2013, has a temporal resolution of 16 days and can be resampled to produce optical 15 m spatial resolution imagery. As such, Landsat 8 data are ideal for large-scale landslide mapping over the past 6 years.

2.2 Methodology

The methodology for manual landslide mapping using Landsat imagery is straightforward. The Landsat imagery can be viewed and downloaded from the USGS EarthExplorer platform. This platform allows the user to identify their region of interest, the products they are interested in, and the level of cloud cover that is acceptable. Selected data can be ordered and downloaded in bulk as .TIF files which are in the WGS_1984_UTM coordinate system. The composition of the Landsat imagery are by default defined by the RGB (red, green, blue) composite frequency bands. However, for landslide mapping it is preferable to alter the red-frequency band to the Near Infrared (NIR) frequency band. This facilitates more efficient landslide mapping as there is a greater difference of NIR-frequency reflection between vegetation and bare earth compared to the red-frequency reflection between vegetation and bare earth. Similarly, the Landsat bands can be used to calculate Normalized Difference Vegetation Index (NVDI) values, which are commonly used to distinguish between bare-earth and vegetation (Joyce et al., 2008). **Figures 1a-c** demonstrates how Landsat 8 imagery with bands NIR/Green/Red can be effectively used to delineate fresh

landslides in a set time interval. In this case, landslides were mapped as polygon shape files using ArcGIS editor tools (note, alternative open source Geographical Information Systems exist i.e. QGIS) by visually comparing pre- and post-monsoon Landsat imagery.

As the Landsat satellites cover several decades, it is possible to quickly build up a detailed history of land sliding in a given region. This information can first be used to visually assess areas of high vulnerability to future landslide hazard. For example, **Fig. 2** shows landslides that have occurred along a small portion of the Araniko Highway, between 1989 and 2018. By overlying these landslide data with infrastructure data, a preliminary visual assessment of the hazard can be conducted. Furthermore, freely available DEMs can be used to extract topographical information on a given area, which can then be used to conduct a more quantitative assessment of the susceptibility vulnerability and risk. Methods for this include regression modelling, frequency ratios and neural networks, as well as machine learning techniques (e.g. Aditian et al., 2018; Chang et al., 2007; Poudyal et al., 2010). These Landsat examples demonstrate that freely available data can be used effectively for the mapping and subsequent analysis of landslide hazard, thus contributing to Nepal's need to adhere to the Sendai Framework.

3. Urban Development utilizing Digital Elevation Models

Globally, over 4.1 billion people are estimated to be living in urban areas. Within Kathmandu valley, estimates of the population vary between 1.5 and 2.5 million, whilst its population growth rate of > 5% is one of the greatest in Asia. The urban area of Kathmandu valley has increased by over 400% over the last three decades (Ishtiaque et al., 2017). A significant portion of this development has been unplanned and unregulated. Kathmandu Valley is affected by a range of natural hazards, including earthquakes, fluvial flooding and landslides, as well as cascading hazards such as fire caused by earthquakes. As such, there is a need to understand the potential impact of natural hazards on the built environment. The following section outlines available open source data sets for Kathmandu, including Digital Elevation Models (DEMs) and geological data, and a methodology for how these data sets can be utilized to provide a preliminary understanding of natural hazards in an urban setting.

3.1 Data sets and methodology

A digital elevation model is a discrete grid of values where each value represents the average surface elevation or relief within that grid. A range of open source Digital Elevation Model (DEM) data exists, most of which require limited data processing to enable a range of analyses to be undertaken. The most commonly used DEMs are:

- Shuttle Radar Topography Mission (SRTM) data, with almost global coverage and a resolution of approximately 30 m available to download from the United States Geological Survey (USGS);
- Advanced Spaceborne Thermal Emission and Reflection Radiometer (ASTER) Digital Elevation Model with almost global coverage and a resolution of approximately 30 m available to download from the USGS;
- Advanced Land Observing Satellite (ALOS) Digital Elevation Model with almost global coverage and a resolution of approximately 30 m available to download from the Japan Aerospace Exploration Agency (JAXA).

More accurate open source DEMs are available, but are often limited in coverage or require significant data processing. For example, Sentinel-1 InSAR data available from the European Space Agency can achieve a reported 1 m resolution, but requires specialist knowledge and data processing to utilize fully. As such, this review focuses on DEMs that require little data processing to be visualized within a Geographical Information System (GIS).

In terms of geological data, relevant information for Kathmandu Valley were obtained from the Nepal Department of Geology and Mines (Shrestha et al., 1998) as GIS Layer files. Required information on landslides and superficial deposits were then extracted and imported into GIS.

3.2 Methodology

Once the relevant data sets were acquired, the ALOS DEM was imported into ArcGIS (alternative open source Geographical Information Systems exist i.e. QGIS). To generate the stream/river network, the hydrology toolset (see www.arcgis.com) and the pre-prescribed steps were undertaken. The river network was then overlaid on to OpenStreetMap population data for Kathmandu Valley (Humanitarian Data Exchange 2019) and the geological and geohazard data of interest (fluvial sediments, unconsolidated sediments and landslides) (Shrestha et al., 1998). Although, these geological, geohazard and

population data were obtained from existing references, where these existing data sources do not exist, it is possible to obtain these data sets from remote sensed multi-spectral data as outlined for landslides in Section 2 and as discussed further in Section 4.

The representations of these different data sets are illustrated in **Figs. 3**, **4** and **5**. **Figure 3** shows the urban and semi urban areas with information related to rivers and historical flood deposits. **Figure 4** shows the urban data with unconsolidated and slightly consolidated sediments that could potentially liquefy during an earthquake. Finally, **Figure 5** shows the urban data with mapped landslides deposits. These analyses provide preliminary insight into how a range of geohazards within Kathmandu Valley interact with the built environment. This illustrates that a significant portion of urban areas are susceptible to flooding and potentially liquefaction during an earthquake, and that with the increasing urbanization of Kathmandu Valley development is encroaching onto areas susceptible to landslides. The utilization of Geographical Information Systems, open source remote sensed data and published data can support our understanding of current hazard and risk scenarios, develop future scenarios, and inform land use planning.

4. Coastal Flood Hazard using Digital Elevation Models and Sentinel-2 data

Over the period 1998-2017, over 1250 storm events killed over 200,000 people and affected over 725 million people (CRED/UNISDR 2017). Currently, approximately 40% of the world's population lives within 100 km of the coast. As population density and economic activity in coastal zones increases, coupled with the impact of climate change, the vulnerability to natural hazards such as storms and tsunamis is likely to increase. Therefore, of critical importance is the understanding of future flood scenarios and the interaction with the built environment. The following section details the available open source data sets, coupled with published historical flood levels, and the methodology to undertake a preliminary analysis of coastal flood hazard.

4.1 Data Sets and Methodology

Multispectral satellite data i.e. from Landsat or Sentinel-2, have almost global coverage, with Landsat having an approximate 16-day temporal coverage from 1984 (Landsat 5), and Sentinel-2 having an approximate 5-day coverage from 2015. Spatial resolution of these data sets vary, but the Sentinel-2 data used within this study have a resolution of 10 m in the Red, Green and

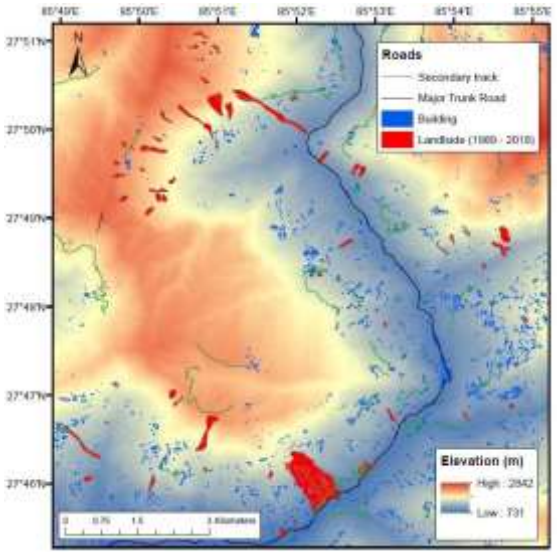

Fig. 2. Landslide data mapped using Landsat 4/5 and 8 imagery between 1989 and 2018 for a section of the Araniko highway alongside road and building obtained from OpenStreetMap (Humanitarian Data Exchange 2019)

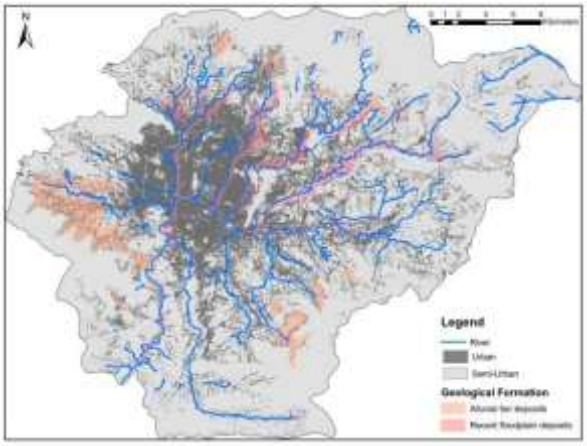

Fig. 3. Map of Kathmandu showing Urban and Semi urban areas, the main rivers extracted from the DEM and mapped alluvial and floodplain deposits. The data illustrates shows the urban areas susceptible to flooding.

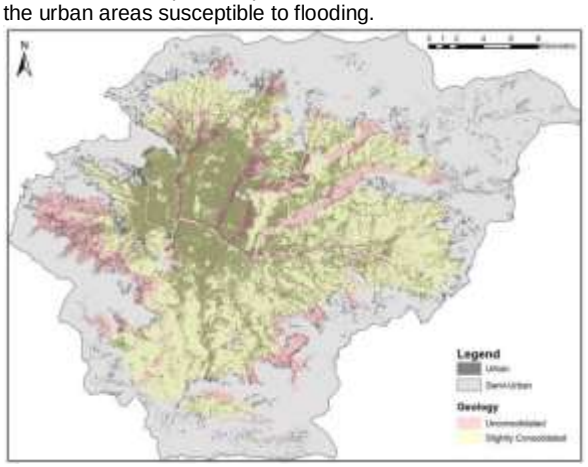

Fig. 4. Map of Kathmandu showing Urban and Semi urban areas overlain by geological data for unconsolidated and semi-consolidated sediments (Shrestha et al., 1998). The data illustrates urban areas potetentially susceptible to liquefaction during an earthquake.

Blue bands. The multispectral element of Sentinel-2 refers to the multispectral imager that measures 13 bands at different wavelengths. These different bands can be combined within a GIS to enable visualization of different components of interest. For example, combining near infra-red, red and green bands can highlight healthy and unhealthy vegetation. Similarly, combining two different short wave infra-red bands and the blue bands can highlight geological change. Other applications can combine different bands to illustrate water bodies, land use and urban areas. **Figure 6** shows a true colour image generated by combining the red, green and blue bands within ArcGIS using the Composite Bands tool. The image shows areas of vegetation, less vegetated areas, small urban areas, the rivers and coast.

In addition to the Sentinel-2 True colour image, an ALOS DEM (**Fig. 7**) was downloaded from JAXA to enable the simulation of the potential flood levels. Flood levels were obtained from historical records, with the inundation level of between 3-4 m for the 2004 boxing day tsunami, which is estimated to have killed 90 people in Myanmar, used to illustrate potential tsunami levels (Satake et al., 2006, Fritz et al., 2008). For storm surges, inundation levels were obtained from Cyclone Nargis, the worst climate related disaster to have impacted Myanmar, with over 130,000, deaths. Cyclone Nargis was estimated to have a storm surge height of up to 5 m, with a 2 m wave height superimposed, flooding was estimated to reach up to 50 km inland (Fritz et al., 2008).

To provide a simplified representation of the flood levels from the 2004 tsunami and the 2008 storm surge, contour levels of 4 m and 7 m, respectively were extracted from the DEM. This method is likely to be an underestimation as it does not consider drawdown run-out or other factors. In essence, the methodology simply identified areas of land up to 4 m and 7 m in elevation. To visualize the inundation levels the extracted contours were overlaid on to the Sentinel-2 imagery and are shown in **Fig. 8**.

From **Fig. 8**, it can be seen that there is little difference between the flood contours for the tsunami and storm surge. This is most likely due to a combination of the small difference in height and the resolution of the DEM. Further discussions on resolution limitations are provided in Section 6. However, despite these limitations, the data allows the visualization of flood levels and their potential impact, showing areas of greater inundation and the impact on urban development. Furthermore, simple analyses similar to the above can be used to support disaster management plans and disaster response by identifying areas most likely to be inundated and areas where access might be difficult due to the impact of an event on the road infrastructure. Indeed, by overlaying

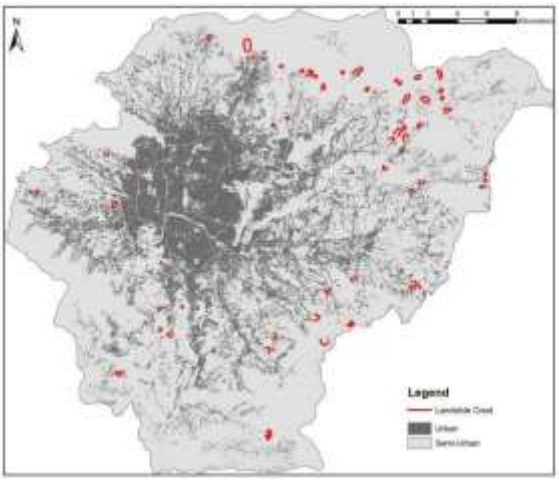

Fig. 5. Map of Kathmandu showing Urban and Semi urban areas overlain by landslide data (Shrestha et al., 1998). The data illustrates urban areas potentially susceptible to landslides during an earthquake

Fig. 6. True colour composite image of a Coastal Zone in Myanmar, produced by combining Sentinel-2 multispectral bands Red, Green and Blue within ArcGIS.

shapefiles of key road locations with a DEM, a topographical road survey could be undertaken to determine which portions of a road might be inundated during a given level of flooding.

5. Seismic risk estimation using fluvial geomorphology

That the landscape is shaped by the underlying tectonic activity has long been known. However, it is now becoming possible to use freely available DEMs, such as

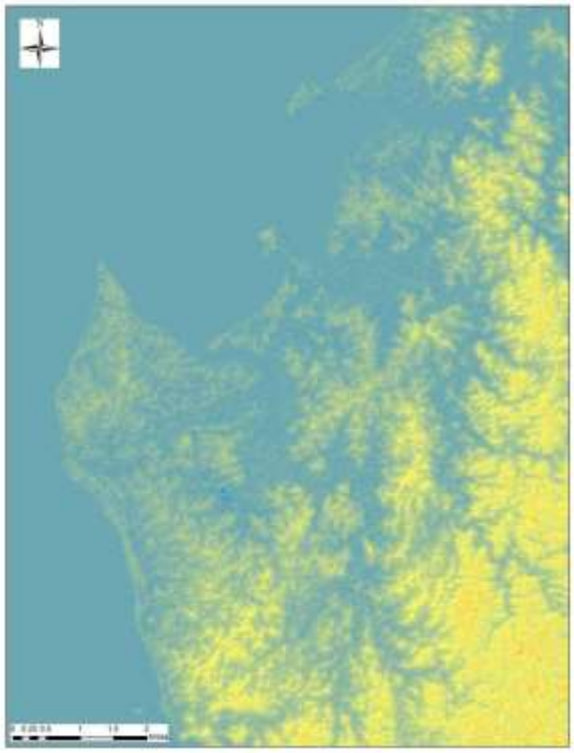

Fig. 7. ALOS Stretched colour ramped Digital Elevation Model (©JAXA) for a Coastal Zone of Myanmar, illustrating the low-lying area adjacent of the coast and potentially susceptible to flooding

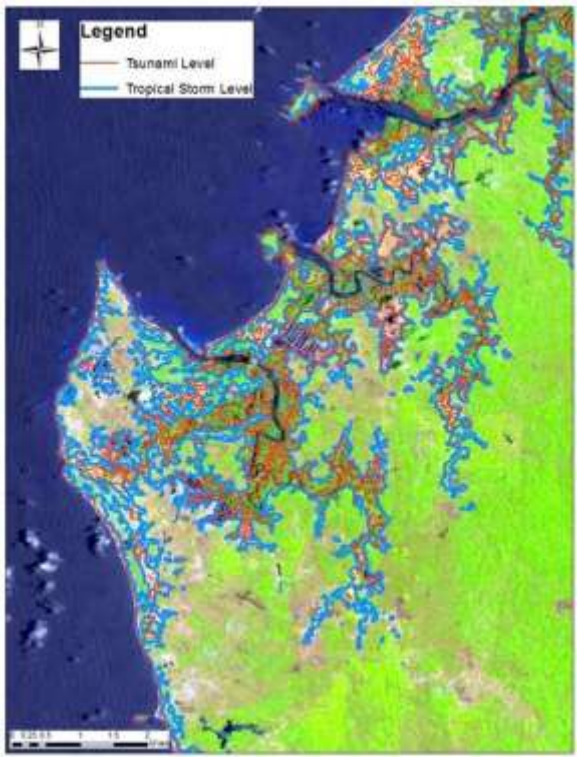

Fig. 8. True Colour Sentinel-2 Imagery with overlay of the 2004 Boxing Day Tsunami and 2008 Cyclone Nargis flood levels shown as a contour levels

those previously described, to derive information from the landscape that can be used to estimate rates of active faulting and/or potential earthquake hazard, specifically through the analysis of the river network. This remote sensing approach is particularly useful in regions were infrastructure or the geopolitical situation may make assessing active faulting through field surveys challenging. Importantly, results of the analyses are not unduly affected by the quality of the available data, so that global 30 m DEMs are a good data source for such analyses (Boulton and Stokes, 2018).

The technique relies upon the fact that in bedrock rivers, the physics of which are explained by the stream power erosion law, the steepness of the river channel is correlated to uplift rate (Snyder et al., 2000). In rivers where erosion is equal to uplift, rivers will have a concave-up shape where the river gets gradually shallower in gradient downstream. However, if a perturbation occurs to the system such as an increase in fault activity causing a relative fall in base-level, the river will be perturbed from steady state forming areas of localized steepness (a knickzone) in the channel and gorge formation in the adjacent hillsides. The upstream extent of this wave of incision is known as the knickpoint and separates the reach of the channel that has responded to the change in boundary conditions from the upstream part, yet to feel the effects of the base-level fall. Information regarding the landscape response is revealed through the extraction of quantitative metrics such as the steepness index, ks, and its integral, chi – X, from a DEM (**Fig. 9**). For a detailed explanation of these concepts the reader is directed to Kirby and Whipple (2012) and Perron and Royden (2013).

Furthermore, linear patterns of knickpoints can reveal the location of concealed faults, and knickpoint height can give information on the likely throw along fault in some cases (Boulton and Whittaker, 2009). The extent of knickpoints combined with topographic lineament analysis can also allow the determination of the length of the fault. In combination with fault geometry scaling laws such as Wells and Coppersmith (1994), these data can then be used to estimate the potential moment magnitude that the fault could generate during an earthquake.

5.1 Methodology

The extraction of topographic metrics as described above was until recently relatively computationally challenging; however, recently a number of open source matlab programmes have been released allowing increasingly quick and accurate analyses to be undertaken with little to no background in computer programming.

Figure 9 shows analyses undertaken on the island of Makira (Solomon Islands). The initial stage of the

analysis, in common with other methods described herein, requires the acquisition of a DEM such as the 30 m SRTM or ALOS datasets. Preliminary data preparation to mosaic individual DEM tiles and project into a projected coordinate system was undertaken in ArcGIS, along with standard landscape visualization methods such as generating hillshade and slope layers. Following data preparation, landscape metrics were extracted using TopoToolBox (Schwanghart and Scherler, 2014) and the Topographic Analysis Kit (Forte, 2019). The TAK allows the user to not only bulk extract vales for the entire river network but also automatically detect knickpoints. The user can also undertake detailed analysis river by river using river long profile, slope-area and Chi-profile graphs in order to make a determination of the precise knickpoint geometry.

For the Solomon Islands, this analysis revealed that a number of the rivers across the island contain steep reaches and knickpoints, and that the island's topography is transiently responding to changes in uplift rate along the adjacent subduction zone (Boulton, 2020).

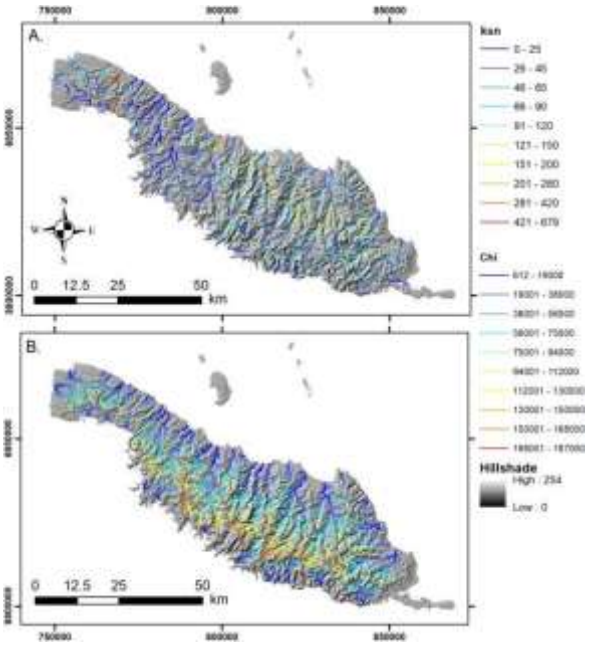

Fig. 9. A) Map of Makira (Solomon Islands) showing the river network shaded by normalized steepness index. B) The same network but symbolised by Chi. Data extracted from the SRTM 30 m DEM.

6. Limitations of Data Sets

The outlined approaches aim to obtain a basic preliminary assessment of natural hazards to support understanding and planning of current and future risk scenarios. Given the methodology is based on open source remote sensed data and scientific literature, there are a range of limitations. Although not exhaustive, some of the main limitations are:

- Resolution of the DEMs used within this study are approximately 30 m. As such, the analysis undertaken i.e. river generation and flood contours, are affected and may not represent the true alignment or level;
- Landsat resolution is in the region of 30 m, which means smaller landslides are not observed in the data set;
- Temporal resolution of the Landsat data is on the order of 16 days. This relatively long return time, combined with issues of cloud cover, can be problematic when trying to distinguish landslides triggered by successive events that occurred in a short time period. For example, in 2015, the Mw 7.8 Gorkha earthquake mainshock, the Mw 7.3 Gorkha aftershock, and the monsoon season, all occurred within a month. As such, delineating which landslides were triggered by which event is challenging with Landsat alone.
- Depending on the analysis undertaken, Sentinel-2 data has a resolution of between 10 m and 60 m. Therefore, features such as urban areas and geology may not fully represent the real world. Furthermore, as processed sentinel-2 looks for contrast (i.e. urban vs vegetated areas), the output may not correctly delineate the different zones or areas of interest.
- Utilising contour levels to illustrate flood levels is an over simplification and does not evaluate the complex interactions of a storm surge or tsunami and the coast. Furthermore, utilizing a single event does not consider all scenarios. Detailed modelling and evaluation of storm surge and tsunami magnitude and return periods (see Boulton and Whitworth, 2018, Whitworth et al, 2004) should be undertaken.

7. Conclusions

Over the twenty-year period 1998-2017, natural disasters have killed over 1.3 million people and impacted over 4.4 million. With ever increasing populations and related development within areas of higher risk, combined with factors such as climate change, indications are that the impact of natural disasters are likely to increase unless affirmative action is undertaken. The Sendai Framework aims to reduce the impact of natural disasters with a stated outcome of "The substantial reduction of disaster risk and losses in lives, livelihoods and health and in the economic, physical,

social, cultural and environmental assets of persons, businesses, communities and countries". This paper focuses on priority 1, understanding disaster risk, linking to the requirement of the UNISDR Resilience Scorecard "to identify, understand and use current and future risk scenarios".

As the requirement for a detailed assessment can be time consuming, costly and difficult to undertake on a large scale, the paper focuses on the use of Open Source data sets to undertaken preliminary/screening assessments to inform our understanding of current and future hazard and risk scenarios and support more detailed target assessments and planning. Four case studies have been utilized to show the feasibility of undertaking large scale assessments;

1. The use of Landsat satellite imagery in the analysis of historical landslide occurrence along the Ariniko Highway, Nepal, showing that through detailed analysis a historical landslide record of 30 years can be created and used to evaluate the impact of landslides on the urban environment and critical infrastructure
2. The role of open source data in an urban setting (Kathmandu) utilising urban land use classification coupled with DEM determined drainage models and geological data. The findings illustrate the susceptibility of the built environment to flooding, liquefaction and landslides. The data can be used to support city planning.
3. The application of digitals data sets in a coastal environment (Myanmar) with the focus on flood hazard. A simple analysis utilizing Digital Elevation Models and Sentinel-2 data can provide a preliminary assessment of the impact of tsunami and storm surges.
4. The use of DEMs in the identification of active faulting and the extraction of landscape metrics that can be used to identify regions of uplift and incision in vulnerable landscapes.

Despite the limitations of the available data, we find that the outputs provide an important preliminary assessment of geohazards, therefore, enabling a focus on areas of high susceptibility and vulnerability while supporting the aims of the Sendai Framework.

References

Aditian, A., Kubota, T., Shinohara, Y., 2018. Comparison of GIS-based landslide susceptibility models using frequency ratio, logistic regression, and artificial neural network in a tertiary region of Ambon, Indonesia.https://doi.org/10.1016/J.GEOMORPH.2018.06.006, Geomorphology, **318**: 101-111.

Boulton, S.J., 2020. Geomorphic response to differential uplift: river long profiles and knickpoints from Guadalcanal and Makira (Solomon Islands). https://doi.org/10.3389/feart.2020.00010, Frontiers in Earth Science, **8**: pp 10.

Boulton S.J. and Stokes M. 2018. Which DEM is best for analyzing fluvial landscape development in mountainous terrains? Geomorphology, **310**: 168-187.

Boulton S.J. and Whittaker, A.C., 2009. Quantifying the slip rates, spatial distribution and evolution of active normal faults from geomorphic analysis: Field examples from an oblique-extensional graben, southern Turkey. Geomorphology, **104**: 299-316.

Boulton, S.J. and Whitworth, M.R., 2018. Block and boulder accumulations on the southern coast of Crete (Greece): evidence for the 365 CE tsunami in the Eastern Mediterranean. Geological Society, London, Special Publications, **456** (1): 105-125.

Chang, K.-T., Chiang, S.-H. and Hsu, M.-L., 2007. Modeling typhoon- and earthquake-induced landslides in a mountainous watershed using logistic regression. Geomorphology, **89**: 335-347, https://doi.org/10.1016/J.GEOMORPH.2006.12.011.

CRED/UNISDR, 2017. Economic Losses, Poverty and Disasters 1988-2017 available at www.emdat.be.

Fritz, H.M., Blount, C.D., Thwin, S., Thu, M.K. and Chan, N., 2009. Cyclone Nargis storm surge in Myanmar. Nature Geoscience, **2** (7): pp 448.

Fortes, A.M., 2019. the topographic analysis kit (TAK) for TopoToolbox. Earth Surface Dynamics, 7 (1): pp.87.

Hartman, C.W., Squires, G., and Squires, G.D. (Eds.), 2006. There is no such thing as a natural disaster: Race, class and Hurricane Katrina. Routledge. Taylor & Francis, 2006, ISBN 0-415-95486-X.

Humanitarian Data Exchange, 2019. Open street map population and infrastructure data acquired from www.humdata.org.

Jones, J.N., Stokes, M., Boulton, S.J., Bennett, G.L. and Whitworth, M.R.Z. 2019, Ongoing cosiemic and post-earthquake landslide impacts on remote trekking infrastructure, Langtang Valley, Nepal. Quarterly Journal of Engineering Geology and Hydrogeology, http://dx.doi.org/10.1144/qjegh2019-048.

Joyce, K.E., Dellow, G.D., Glassey, P.J., 2008. Assessing Image Processing Techniques for Mapping Landslides, in: IGARSS 2008-2008 IEEE International Geoscience and Remote Sensing Symposium. IEEE, https://doi.org/10.1109/IGARSS.2008.4779224: **II**:1231-1234.

Kirby E. and Whipple K.X. 2012. Expression of active tectonics in erosional landscapes. Journal of

Structural Geology, DOI: 10.1016/j.jsg.2012.07.009, **44**: 54-75.

Ishtiaque, A., Milan S., and Netra, C., 2017. Rapid urban growth in the Kathmandu Valley, Nepal: Monitoring land use land cover dynamics of a Himalayan city with Landsat imageries. Environments, **4**, (4): 72-88

Poudyal, C.P., Chang, C., Oh, H.-J. and Lee, S., 2010. Landslide susceptibility maps comparing frequency ratio and artificial neural networks: A case study from the Nepal Himalaya. Environ. Earth Sci., https://doi.org/10.1007/s12665-009-0426-5, **61**: 1049-1064.

Perron, J.T. and Royden, L., 2013. An integral approach to bedrock river profile analysis. Earth Surface Processes and Landforms, **38** (6): 570-576.

Satake, K., Aung, T.T., Sawai, Y., Okamura, Y., Win, K.S., Swe, W., Swe, C., Swe, T.L., Tun, S.T., Soe, M.M. and Oo, T.Z., 2006. Tsunami heights and damage along the Myanmar coast from the December 2004 Sumatra-Andaman earthquake. Earth, planets and space, **58** (2): 243-252.

Schwanghart, W. and Scherler, D., 2014. TopoToolbox 2–MATLAB-based software for topographic analysis and modeling in Earth surface sciences. Earth Surface Dynamics, **2** (1): 1-7.

Shrestha, O.M., Koirala, A., Karmacharya, S.L., Pradhananga, U.B., Pradhan, P.M. and Karmacharya R., 1988. Environmetal geological Map of the Kathmandu Valley. Department of Geology and Mines, Nepal.

Snyder, N.P., Whipple, K.X., Tucker, G.E. and Merritts, D.J., 2000.

Stream profiles in the Mendocino triple junction region, northern California. GSA Bulletin **112**: 1250-1263.

UN, 2017. Sendai Framework for Disaster Risk Reduction 2015-2030. United Nations Office for Disaster Risk Reduction, Pages 32

UNDRR, UN, 2017. Office for Disaster Risk Reduction, Disaster Resilience Scorecard for Cities, May 2017: pages 52

Wells, D.L. and Coppersmith, K.J., 1994. New empirical relationships among magnitude, rupture length,rupture width, rupture area, and surface displacement. Bulletin of the seismological Society of America, **84** (4): 974-1002.//

Whitworth, M., Poulsom, A. and Hunt, T., 2004. An assessment of the hazard posed by storm surges in the Tamar Estuary. Geoscience in south-west England, **11**: 00-11.

Woodcock, C.E., Allen, R., Anderson, M., Belward, A., Bindschadler, R., Cohen, W., Gao, F., Goward, S.N., Helder, D., Helmer, E., Nemani, R., Oreopoulos, L., Schott, J., Thenkabail, P.S., Vermote, E.F., Vogelmann, J., Wulder, M.A. and Wynne, R., 2008. Free access to Landsat imagery. Science, https://doi.org/10.1126/science.320.5879.1011a, **320**: 1011-1011

Xu, C., Tian, Y., Zhou, B., Ran, H. and Lyu, G., 2017. Landslide damage along Araniko highway and Pasang Lhamu highway and regional assessment of landslide hazard related to the Gorkha, Nepal earthquake of 25 April 2015. Geoenvironmental Disasters, https://doi.org/10.1186/s40677-017-0078-9, **4**: 14.

Symbols and abbreviations

ALOS	Advanced Land Observing Satellite
ASTER	Advanced Spaceborne Thermal Emission and Reflection Radiometer
DEM	Digital Elevation Models
GDP	Gross domestic product
GIS	Geographical Information System
JAXA	Japan Aerospace Exploration Agency
NASA	National Aeronautics and Space Administration
NIR	Near Infrared
NVDI	Normalized Difference Vegetation Index
RGB	red, green, blue
SCL	Scan Line Corrector
SRTM	• Shuttle Radar Topography Mission
USGS	United States Geological Survey